DC-Bias Effects on Sputtered PZT pMUTs with High Transmit and Receive Sensitivities in Immersion for Imaging applications

Mantalena Sarafianou*, David Sze Wai Choong*, Duan Jian Goh*, Jihang Liu*, Srinivas Merugu*, Qing Xin Zhang*, Peter H. K. Chang*, Domenico Giusti†, Laura Castoldi†, Filippo D'Ercoli†, Riccardo Tacchini†, Alberto Leotti‡, Dao Hao Sim‡, Alessandro Stuart Savoia§, and Joshua En-Yuan Lee*
Email: mantalena_sarafianou@ime.a-star.edu.sg,
*Institute of Microelectronics (IME), Agency for Science, Technology and Research (A*STAR), Singapore,
†STMicroelectronics, Italy,
‡ STMicroelectronics, Singapore,
§ Roma Tre University, Italy

***Abstract*—This work reports a 7.5MHz sputtered Lead Zirconate Titanate (PZT) piezoelectric micromachined ultrasonic transducer (pMUT) array that demonstrates both strong transmit (9.3kPa/V/mm^2) and receive performance (6.5V/MPa) characterized in immersion without signal amplification and within a 5mm^2 aperture. This paper presents yet higher RX sensitivities for the proposed device even with a direct connection to an oscilloscope. We elucidate the effect of DC bias on the acoustic transmit (TX) and receive (RX) characteristics of PZT pMUTs, and how these could be tuned to increase the performance of the pMUTs. The device was fabricated at wafer-scale in our 8-inch line, which is capable of physical vapor deposition (PVD) of high quality PZT.**

***Index Terms*—pMUT, physical vapour deposition, Lead Zirconate Titanate, transmit sensitivity, receive sensitivity, ultrasonic imaging**

I. Introduction

To-date, ultrasound has been explored for a wide range of applications including among others: ranging [1]–[3], medical imaging [4], [5], non-destructive testing (NDT) [6], mid-air haptics [7] and gesture recognition [8].

Compared to conventional ultrasonic transducers (i.e., bulk piezolectric ceramics), which have been traditionally used in the above applications, piezoelectric micromachined ultrasonic transducers (pMUTs) have certain advantages: small size, low actuation voltage and a flexural membrane (for generating and receiving ultrasound waves) which is much softer than rigid ceramics, resulting in better impedance matching and transmission efficiency [9].

Specifically, for the application of ultrasonic imaging, high transmit (TX) and receive (RX) sensitivity are vital considerations. Yet there is commonly a trade-off between the two parameters: Lead Zirconate Titanate (PZT) being strong on TX while AlN is deemed as stronger in RX (based on a higher FOM of e^{31f}/ϵ_r). AlN PMUTs have been demonstrated at wafer-scale [10], [11] and championed for their perceived advantage in RX sensitivity over other materials. By fabricating the pMUTS on CMOS, [10], [11] reported an RX sensitivity of 5.9V/MPa (including the gain of an integrated frontend amplifier) and an estimated bandwidth of 33%. The low e_{31f} piezoelectric constant (this coefficient quantifies the volume change when a piezoelectric material is subject to an electric field, or the polarization on the application of stress) of AlN results in poor transmit (TX) performance (approximately 1kPa/V), excludes these devices from reaching MPa outputs needed for imaging deep into the body. In [12], an increased TX sensitivity circa 2 times with a 15V DC bias voltage (V_b) was reported along with a piezoelectric constant e_{31f} value of -13.5C/m^2.

In this work, a 7.5Hz sputtered PZT piezoelectric micromachined ultrasonic transducer (pMUT) array is reported, which can deliver approximately 200kPa output in immersion using only 5.5Vpp within a 5mm^2 aperture. The pMUT's receive (RX) sensitivity is equivalent to 6.5V/MPa without any form of amplification, comparable to the best AlN-based pMUTs known for high RX sensitivity. In addition, the impressive TX sensitivity of 9.3kPa/V/mm^2 is highly attractive for imaging applications. In this paper, the proposed pMUT design is first described (Section II) followed by discussion on the experimental setups considered in this work for device characterisation (Section III). In Section IV the experimental results are presented and argued with conclusions drawn in Section V.

II. Description of pMUT Design

The proposed pMUT array design depicted in Figure1 has an aperture of $2.1 \times 2.1mm^2$ within a $3 \times 3mm^2$ chip, consisting of 18×18 membranes (each 80μm wide and designed to resonate at 7MHz in air). The pitch between the membranes is 120μm. Each membrane comprises a 2μm-thick sputtered PZT on a 4μm-thick silicon device layer. The chip was wire bonded to a custom-designed PCB fitted to a Perspex tube to contain the fluid around the chip for testing in immersion (i.e., water).

The TX and RX sensitivities are directly proportional to the material properties, namely the constant e_{31f} and the ratio e_{31f}/ϵ_{33f} respectively, where ϵ_{33f} corresponds to the film relative permittivity. Based on the theoretical curve of e_{31f} reported by Caro M. A. et al. in [13], ScAlN with 20% Sc concentration would result in a value of -1.5C/m^2, with AlN having -1C/m^2 [14]. In contrast, our PZT has a substantially higher e_{31f} of -15C/m^2 [14], resulting in a high TX sensitivity and a moderate RX sensitivity.

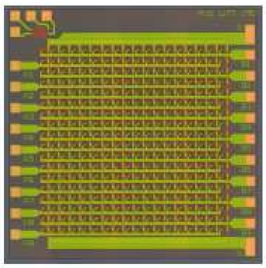

Fig. 1. Top-view image of PZT PMUT array chip.

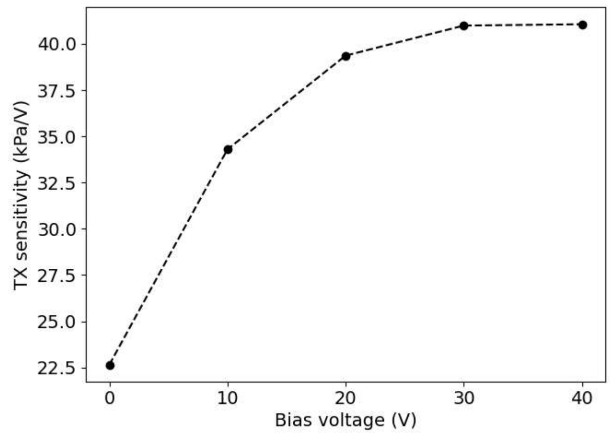

Fig. 2. TX sensitivity as a function of DC bias voltage.

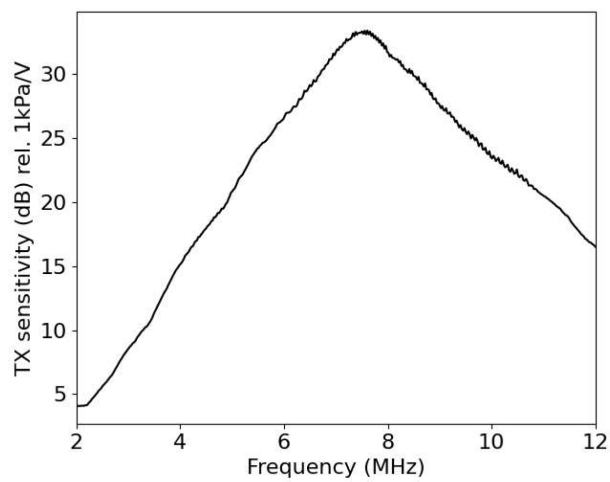

Fig. 3. TX sensitivity as a function of frequency.

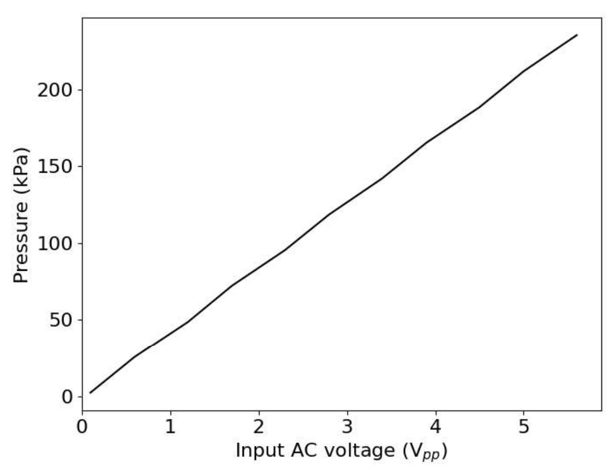

Fig. 4. Pressure as a function of input AC voltage.

III. Experimental Setup

The full array of pMUTs was characterized in immersion considering two testing setups as discussed in the following subsections.

A. TX Sensitivity Measurement Setup

The chip was connected to a bias tee, which took two inputs for the actuation of the die: (i) a 10-cycle sinusoidal waveform was set on a signal generator, and (ii) a DC voltage was set via a power supply. A needle hydrophone was positioned at a distance of 2cm away from the pMUT chip and also immersed in water to measure the line-of-sight (LoS) signal. The received signal was captured by an oscilloscope with all the lab equipment being controlled from a laptop.

B. RX Sensitivity Measurement Setup

In this case, a 6.5MHz Olympus broadband transducer and impulse generator were used to obtain the RX characteristics of the pMUT considering a pitch-catch configation in immersion. Initially, the transducer was placed 2cm away from the calibrated needle hydrophone and was actuated with a 160V$_{pp}$ impulse. The FFT of the impulse response measured with the hydrophone was computed and used to calibrate the broadband transducer.

The calibrated broadband transducer was then placed in immersion 2cm away from the pMUT device and the RX sensitivity was computed as the ratio of the FFT of the RX signal measured by the broadband transducer divided by the FFT of RX pressure. The bias tee, used in this configuration allowed for the DC bias voltage to be altered from zero to the optimum value.

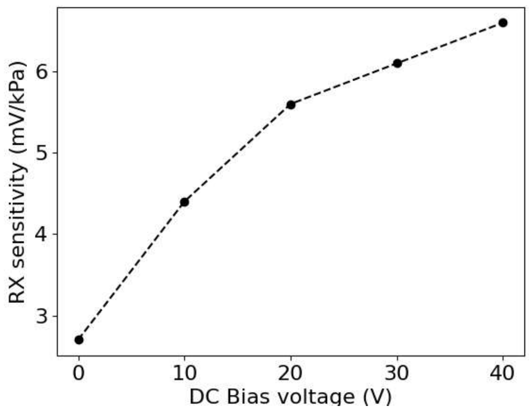

Fig. 5. RX sensitivity as a function of DC bias voltage.

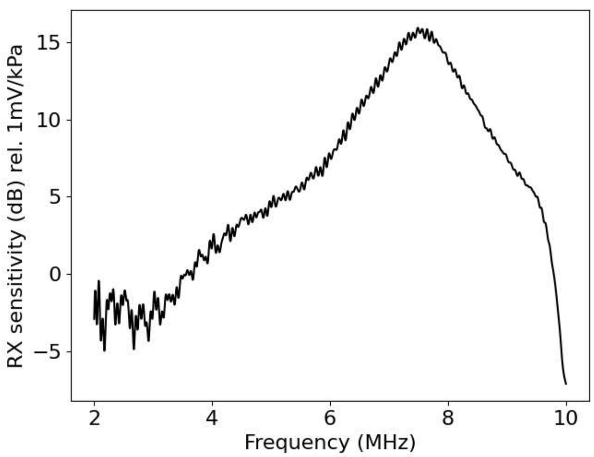

Fig. 6. RX sensitivity as a function of frequency.

IV. Analysis of Results

Figure 2 depicts the TX sensitivity for the pMUT die. Through the characterisation of the pMUT array in immersion, the TX sensitivity improves with increasing DC bias, saturating at the optimum output level of 41kPa/V from 30V onwards as observed in Fig. 2. The measured -3dB bandwidth is 20% with a high TX sensitivity at 30V bias as observed in Figure 3. Figure 4 shows the linearity of the TX output with V_{pp} input, delivering a pressure greater than 200kPa with only $5V_{pp}$.

The RX sensitivity is finally measured as a function of DC bias in the pitch-catch configuration with a broadband ultrasound source as depicted in Figure 5. It can be observed from this figure that the peak response increases with the bias level, reaching to 6.5V/MPa at 40V. Figure 6 shows the RX frequency response at 30V with -3dB bandwidth of 20%. It is worth noting that RX measurements were made with direct cable connections to an oscilloscope to illustrate the robustness of the PZT pMUTs.

V. Conclusions

This work reported a 7.5MHz sputtered PZT pMUT array that delivers 200kPa output in immersion with only $5V_{pp}$ within a $5mm^2$ aperture. The device was fabricated at wafer-scale in our 8-inch line, which is capable of physical vapor deposition (PVD) of high quality PZT is highly attractive for imaging applications. The pMUT's receive (RX) sensitivity is 6.5V/MPa (with no amplification gain), on par with the best AlN-based pMUTs known for high RX sensitivity, whereas the device achieves an impressive TX sensitivity of $9.3kPa/V/mm^2$. The pMUT demonstrates an impressive -3dB bandwidth in the RX mode of 20%. The effect of DC bias on the acoustic TX and RX characteristics of PZT pMUTs was discussed and the means by which these could be tuned to increase the performance of the pMUTs.

Acknowledgment

This research was supported by A*STAR under "Piezo Specialty Lab-in-Fab" (Grant No. I1901E0050).

References

[1] M. Sarafianou, D. J. Goh and D. S. Wai Choong, "A Time-of-Flight (ToF) estimation algorithm for ranging using Silicon-On-Nothing pMUTs," 2022 IEEE International Ultrasonics Symposium (IUS), Venice, Italy, 2022, pp. 1-4, doi: 10.1109/IUS54386.2022.9957846.

[2] Y. Koh, D. S.W. Choong, D. S.-H. Chen, D. J. Goh, S. Ghosh, J. Sharma, S. Merugu, F. Quaglia, M. Ferrera, A. S. Savoia et al., "High resolution, high frequency ultrasonic ranging in air with pmuts," in 2021 IEEE International Ultrasonics Symposium (IUS). IEEE, 2021, pp. 1–4.

[3] Z. Qiu, Y. Lu, and Z. Qiu, "Review of ultrasonic ranging methods and their current challenges," Micromachines, vol. 13, no. 4, p. 520, 2022.

[4] M. Sarafianou, D. S. W. Choong, D. J. Goh, D. S. -H. Chen and Z. Yao, "A CSM/TFM imaging scheme for Silicon-On-Nothing ScAlN pMUT arrays," 2022 IEEE International Ultrasonics Symposium (IUS), Venice, Italy, 2022, pp. 1-4, doi: 10.1109/IUS54386.2022.9958238.

[5] W. Lee and Y. Roh, "Ultrasonic transducers for medical diagnostic imaging," Biomedical engineering letters, vol. 7, no. 2, pp. 91–97, 2017.

[6] C. Holmes, B. W. Drinkwater, and P. D. Wilcox, "Post-processing of the full matrix of ultrasonic transmit–receive array data for non-destructive evaluation," NDT & e International, vol. 38, no. 8, pp. 701–711, 2005.

[7] I. Rakkolainen, E. Freeman, A. Sand, R. Raisamo, and S. Brewster, "A survey of mid-air ultrasound haptics and its applications," IEEE Transactions on Haptics, vol. 14, no. 1, pp. 2–19, 2020.

[8] R. J. Przybyla, H. -Y. Tang, S. E. Shelton, D. A. Horsley and B. E. Boser, "12.1 3D ultrasonic gesture recognition," 2014 IEEE International Solid-State Circuits Conference Digest of Technical Papers (ISSCC), San Francisco, CA, USA, 2014, pp. 210-211.

[9] B. T. Khuri-Yakub and O¨ mer Oralkan, "Capacitive micromachined ultrasonic transducers for medical imaging and therapy," Journal of Micromechanics and Microengineering, vol. 21, no. 5, p. 054004, April, 2011.

[10] E. Ledesma, I. Zamora, F. Torres, A. Uranga, V. Tzanov, S. Bhd, "ALN Piezoelectric Micromachined Ultrasonic Transducer Array Monolothically Fabricated on Top of Pre-Processed CMOS Substrates", in Proceedings of the 2019 20th International Conference on Solid-State Sensors, Actuators and Microsystems & Eurosensors XXXIII (TRANSDUCERS & EUROSENSORS XXXIII), Berlin, Germany, 23–27 June 2019, pp. 655–658.

[11] I. Zamora, E. Ledesma, A. Uranga, N Barniol, "Miniaturized $0.13-\mu$m CMOS Front-End Analog for AlN PMUT Arrays", Sensors 2020, 20, 1205.

[12] C. Cheng, T. Peters, A. Dangi, S. Agrawal, H. Chen, S.-R. Kothapalli, S. Trolier-McKinstry, "Improving PMUT Receive Sensitivity via DC Bias and Piezoelectric Composition", Sensors 2022, 22, 5614.

[13] Caro MA, Zhang S, Riekkinen T, Ylilammi M, Moram MA, Lopez-Acevedo O, Molarius J, Laurila T. Piezoelectric coefficients and spontaneous polarization of ScAlN. J Phys Condens Matter. 2015 Jun 24;27(24):245901. Epub 2015 May 22. Erratum in: J Phys Condens Matter. 2015 Jul 15;27(27):279602.

[14] Paul Muralt (1997) Piezoelectric thin films for mems, Integrated Ferroelectrics, 17:1-4, 297-307.